



The chemical reactivity of a known anti-psoriasis drug. Part 1: Further insights into the products resulting from oxidative cleavage

Alan M. Jones[†], Magali M. Lorion[†], Tomas Lebl, Alexandra M.Z. Slawin, Douglas Philp, Nicholas J. Westwood^{*}

School of Chemistry and Biomedical Sciences Research Complex, University of St Andrews, St Andrews, Fife KY16 9ST, Scotland, UK

ARTICLE INFO

Article history:

Received 30 September 2009

Received in revised form 28 September 2010

Accepted 18 October 2010

Available online 10 November 2010

Keywords:

Heterocycle

Oxidative fragmentation

Macrocycle

VT NMR analysis

Mechanism

ABSTRACT

The oxidative cleavage of the known anti-psoriasis drug **1** to give **2** has been reported previously. Due to the importance of accessing medium-sized ring containing systems via oxidative cleavage, this reaction has been revisited revealing additional information about the structure of **2**. Alternative reaction products were identified when the reaction was carried out in the presence of water. The conversion of **1** to **2** has also been carried out using ruthenium tetroxide. A detailed variable temperature NMR and computational study of the restricted rotation of the *N*-aryl ring in **2** is presented.

© 2010 Elsevier Ltd. All rights reserved.

1. Introduction

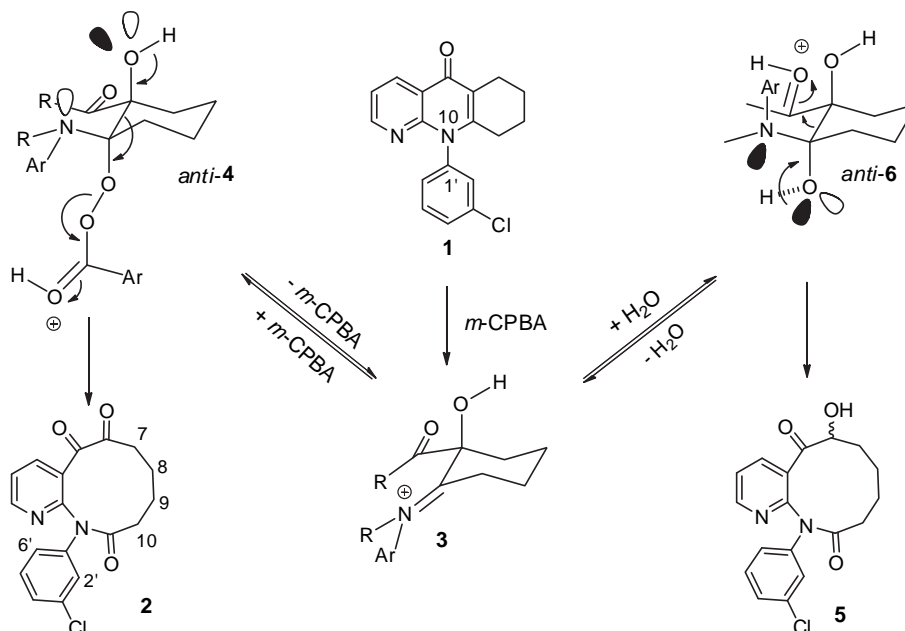
The preparation of compounds containing medium-sized ring systems continues to provide a considerable synthetic challenge. One approach that has proved a particularly robust method of accessing medium-sized rings is the oxidative cleavage of bicyclic ring systems.¹ Once formed, the presence in these systems of a number of functional groups in close proximity often results in the restricted interconversion of ring conformers leading, in some cases, to atropisomerism.²

As a result of our interest in reaction sequences that deliver medium-sized rings using oxidative cleavage reactions, our attention was drawn to the anti-psoriasis drug, 10-(3-chlorophenyl)-6,8,9,10-tetrahydrobenzo[*b*][1,8]naphthyridin-5(7*H*)-one **1** (Scheme 1). In particular, the *m*-CPBA mediated cleavage of the central double bond in **1** to afford **2** has been reported.³ **1** is also of interest from a stereochemical perspective, as it possesses a stereogenic axis due to restricted rotation about the *N*(10)–*C*(1') bond and isolation of the short-lived enantiomers of **1** has been achieved by HPLC using a chiral stationary phase.⁴ The oxidative fragmentation of **1** was proposed to occur via reaction of a second equivalent of *m*-CPBA with iminium ion **3**,³ which may result from

opening of an initially formed epoxide. Attack of the second equivalent of *m*-CPBA was proposed to occur from the opposite face to the hydroxyl functional group in **3** leading to the *anti*-arrangement of the alcohol and the peroxyester groups shown in *anti*-**4** (Scheme 1). Subsequent Grob-fragmentation⁵ of **4** was then suggested to lead to **2** as shown. Interestingly, the ¹H NMR spectrum reported for **2** included diastereotopic protons that were assigned to methylene groups that were remote from the *N*(12)–*C*(1') stereogenic axis (*C*7 and *C*8 in **2**, Scheme 1). Furthermore, an experiment was described in support of the proposed mechanism. **1** was reported to give **5**, via **3** and *anti*-**6** (Scheme 1), when the reaction was carried out in the presence of only 1 equiv of *m*-CPBA and a large excess of water. The proposed formation of **5** was also interesting as **5** might be expected to contain at least one non-classical stereogenic element in addition to its classical stereogenic centre and several issues relating to stereo- and potentially regiochemical control arise in this reaction. To explore this further, we decided to revisit the oxidative fragmentation of **1** by *m*-CPBA and other reagents. Part I of this study details the results of our attempts to prepare **5** and a detailed study of the rotation of the *N*-aryl ring about the *N*(12)–*C*(1') bond in **2**. In the following paper,⁶ we present the synthesis and analysis of ring-expanded analogues of **2**. Part II describes a detailed NMR and computational study of the non-classical stereogenic element associated with the medium-sized ring present in **2** and its analogues.⁶

^{*} Corresponding author. E-mail address: njw3@st-andrews.ac.uk (N.J. Westwood).

[†] These authors contributed equally.



Scheme 1. A proposed³ rationalisation of the formation of **2** and **5**.

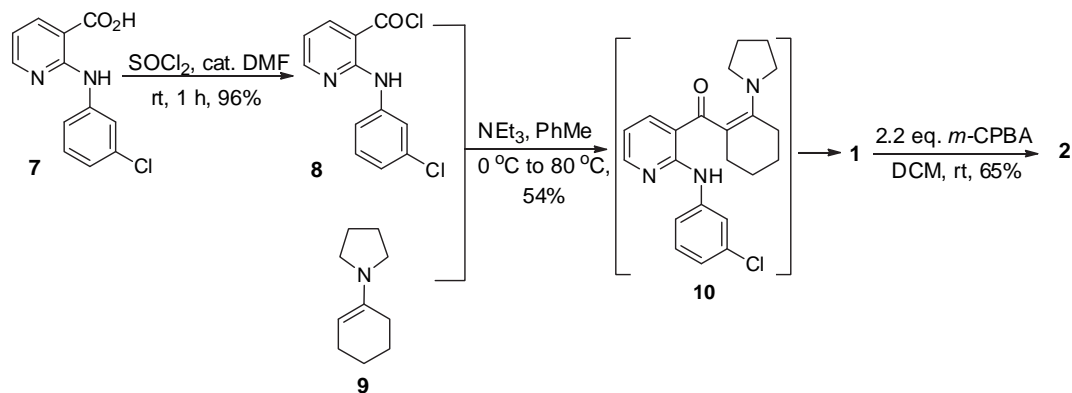
2. Results and discussion

In order to repeat the reported oxidative cleavage reactions with *m*-CPBA, **1** was prepared from **7** by reaction of **8** with commercially available **9** in accordance with literature precedent (Scheme 2).⁷ This reaction probably proceeds via the initial formation of **10** followed by an intramolecular transamination reaction. **1** was then subjected to the previously reported oxidative cleavage conditions to afford **2** in an analogous yield to that previously reported (65% cf. 75%).⁸ The structure of our sample of **2** was confirmed by X-ray crystallographic studies.⁹

Analysis of our sample of **2** in CDCl₃ by ¹H NMR spectroscopy at 293 K revealed a set of aliphatic signals corresponding to diastereotopic protons, as expected. These signals were assigned to the protons of the four methylene carbons in **2** (C7, C8, C9 and C10, Scheme 1). A detailed analysis using 2D NMR experiments, including ¹H,¹H-COSY, ¹H,¹³C-HSQC and ¹H,¹³C-HMBC¹⁰ led us to a different assignment of these signals compared to the original report³ (Fig. 1A). Further analysis of **2** was carried out using variable temperature NMR techniques. These experiments were carried out in toluene-*d*₈ to extend the range of temperatures that could be accessed compared to studies in deuteriochloroform. When the ¹H NMR spectrum was recorded at 223 K, two sets of signals in a ratio of 1:0.7 were visible in the aromatic region of the spectrum (Fig. 1B (i)). The two sets of signals were assigned to two rotamers resulting

from restricted rotation about the N(12)–C(1') bond on the basis of a 2D EXSY experiment.¹⁰ Fig. 1B(i) shows the dramatic differences in chemical shifts experienced by the C2' (signals labelled 2'a and 2'b, Scheme 1 for numbering system) and C6' (6'a and 6'b) protons in the two rotameric forms as well as the two signals assigned to the C7-diastereotopic protons in **2**. Warming the sample to 293 K resulted in coalescence of the signals corresponding to all the aromatic protons whereas both at this temperature and at 363 K no coalescence of the signals corresponding to the C7-diastereotopic protons was observed despite the fact that the frequency difference between the two C7 signals ($\Delta\nu=515$ Hz) is comparable to that observed at 233 K for the C2' and C6' protons ($\Delta\nu=496$ and 419 Hz, respectively).

These variable temperature NMR studies indicated that **2** possesses (at least) one additional stereogenic axis due to restricted bond rotation in the medium-sized ring. In addition, it is clear that the activation barrier associated with this additional dynamic process is higher than that associated with the restricted rotation about the N(12)–C(1') bond in **2**. A detailed discussion of this observation is provided in the following paper in this issue.⁶ Here, as restricted rotation about the N(12)–C(1') bond in **1** enabled isolation of the two enantiomeric atropisomers of **1,4** it was decided to investigate the restricted rotation about the N(12)–C(1') bond in **2** in more detail. The rate constants for restricted rotation about the N(12)–C(1') bond in **2** were determined by lineshape analysis of the C2' and/or C6'



Scheme 2. Synthesis of **1** and the corresponding medium-sized ring containing compound **2**.

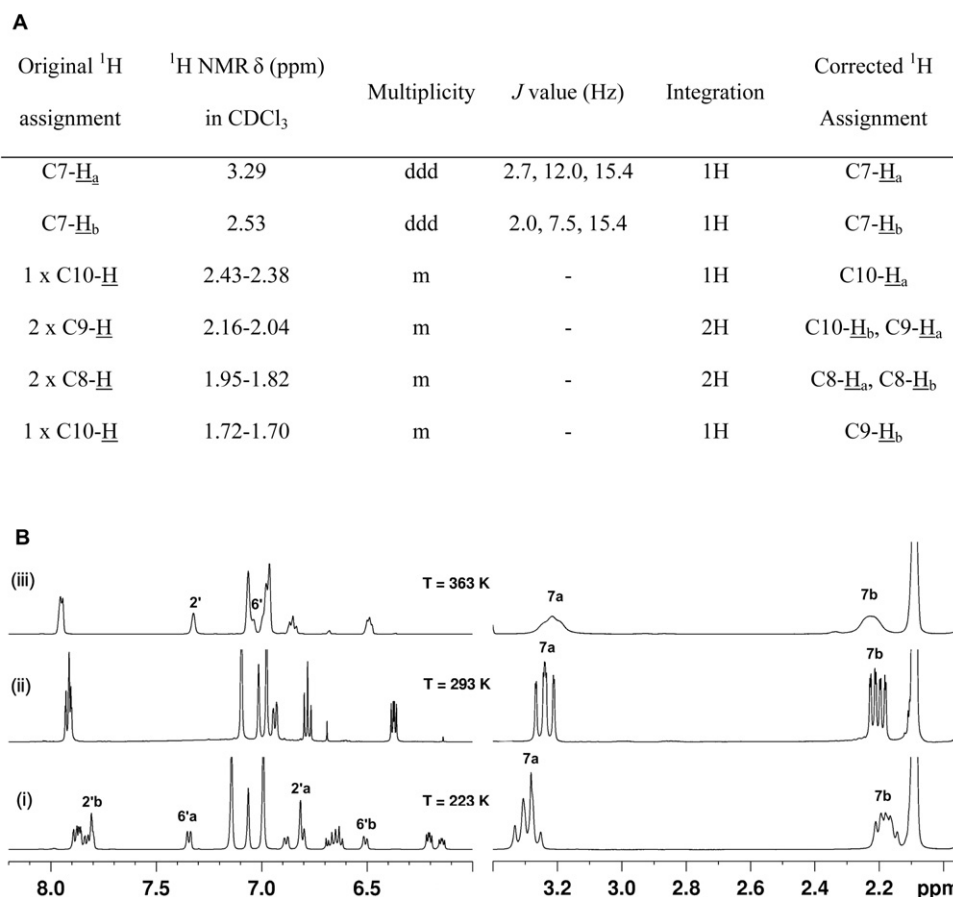


Fig. 1. **A** The reported³ assignment of the aliphatic region of the ^1H NMR spectrum of **2** and the corrected assignment; **B** Comparison of selected regions of the aliphatic and aromatic region of the ^1H NMR (500 MHz) spectrum of **2** recorded in toluene- d_8 at (i) 223, (ii) 293 and (iii) 363 K.

proton resonances in ^1H NMR spectra recorded between 223 and 273 K. In this temperature range the dynamic process associated with the medium-sized ring was in the slow exchange limit and did not contribute to broadening of resonances in the aromatic region. The temperature dependence of the experimentally determined rate constants was used to determine the activation parameters by fitting the experimental data to the Eyring equation. The plots of $\ln(k/T)$ against $1/T$ showed a good overall linear dependence (Fig. S7)¹⁰ and the resulting activation parameters ΔG^\ddagger_{298} , ΔH^\ddagger_{298} and ΔS^\ddagger_{298} were 55.6 kJ mol^{-1} , 56.1 kJ mol^{-1} and $1.7 \text{ kJ K}^{-1} \text{ mol}^{-1}$, respectively. A half life for this dynamic process was therefore calculated to be $3.11 \times 10^{-4} \text{ s}$ at 298 K. Interestingly, the Gibbs free energy of activation (ΔG^\ddagger_{298}) for racemisation of **1**, a process that involves the analogous rotation about the $N(12)$ – $C(1')$ bond, was determined by dynamic high-performance liquid chromatography to be 88.7 kJ mol^{-1} with a corresponding half life of 3.5 min ⁴ Whilst different techniques were used to determine the two ΔG^\ddagger_{298} values, the clearly increased barrier to this rotation in **1** compared to **2**, whilst perhaps not surprising, was of interest to us. To investigate this further, the energy profile for rotation about the $N(12)$ – $C(1')$ bond in **2** was calculated at the RM1 level of theory. This revealed two preferred low energy orientations for the chlorophenyl ring (Fig. 2A). Both of these rotamers were also found in the X-ray structure of **2** (Fig. 2B). Calculation of the ground state structures at the B3LYP/6-31G** level of theory afforded geometries that were in good agreement with the structures obtained experimentally. Selected torsion angles for the experimentally determined and calculated structures are shown for comparison in Fig. 2C.

The energy of structure (ii) (Fig. 2A) was calculated to be only 0.37 kJ mol^{-1} lower than that of the rotameric form (i). This is in

excellent agreement with the 1:0.7 ratio of rotamers observed in the ^1H NMR analysis of **2** at 223 K.¹⁰ Furthermore, the ^1H NMR analysis of **2** at 223 K shows that in the most abundant rotamer the chemical shift of the H2' proton is lower and the chemical shift of proton H6' is higher than the same signals in the less abundant rotamer by (–) 0.99 and (+) 0.84 ppm, respectively.¹⁰ The calculated chemical shift differences (B3LYP/6-31G** level of theory) associated with the H2' and H6' signals between the computationally predicted more stable rotamer (ii) and the less stable rotamer (i) are smaller ((–) 0.64 and (+) 0.61 ppm) but show the same trend.¹⁰

The two transition states that connect rotamers (i) and (ii) with torsional angles ($C12a$ – $N12$ – $C1'$ – $C2'$) of -17.98° and 161.15° , respectively, were located using semi-empirical RM1 method and the geometries were refined at B3LYP/6-31G** level of theory (Fig. 2D). In addition, the calculations showed that the two transition states have nearly the same energy ($\Delta E_{TS1-TS2} = 0.45 \text{ kJ mol}^{-1}$). The calculated geometries (Fig. 2D) indicate that in order to pass through the transition states, the chlorophenyl ring is forced to adopt an orientation in which it is nearly perpendicular with respect to the pyridine ring ($C4a$ – $C12a$ – $N12$ – $C1' = -104^\circ$ in (iii)). The calculated enthalpy of activation of the process (ΔH^\ddagger_{298} 61.0 kJ mol^{-1}) for **2** is only slightly higher than the experimentally determined one (ΔH^\ddagger_{298} 56.1 kJ mol^{-1}). By reorienting the chlorophenyl ring in **2**, a process, that is, not possible in **1**, rotation about the $N(12)$ – $C(1')$ bond is facilitated by avoiding interactions with the lone pair on the pyridine nitrogen and/or the C10 methylene group. The amide bond remains trans throughout aryl ring rotation with the $C12a$ – $C12$ – $C11$ – $C10$ torsional angle remaining approximately constant.

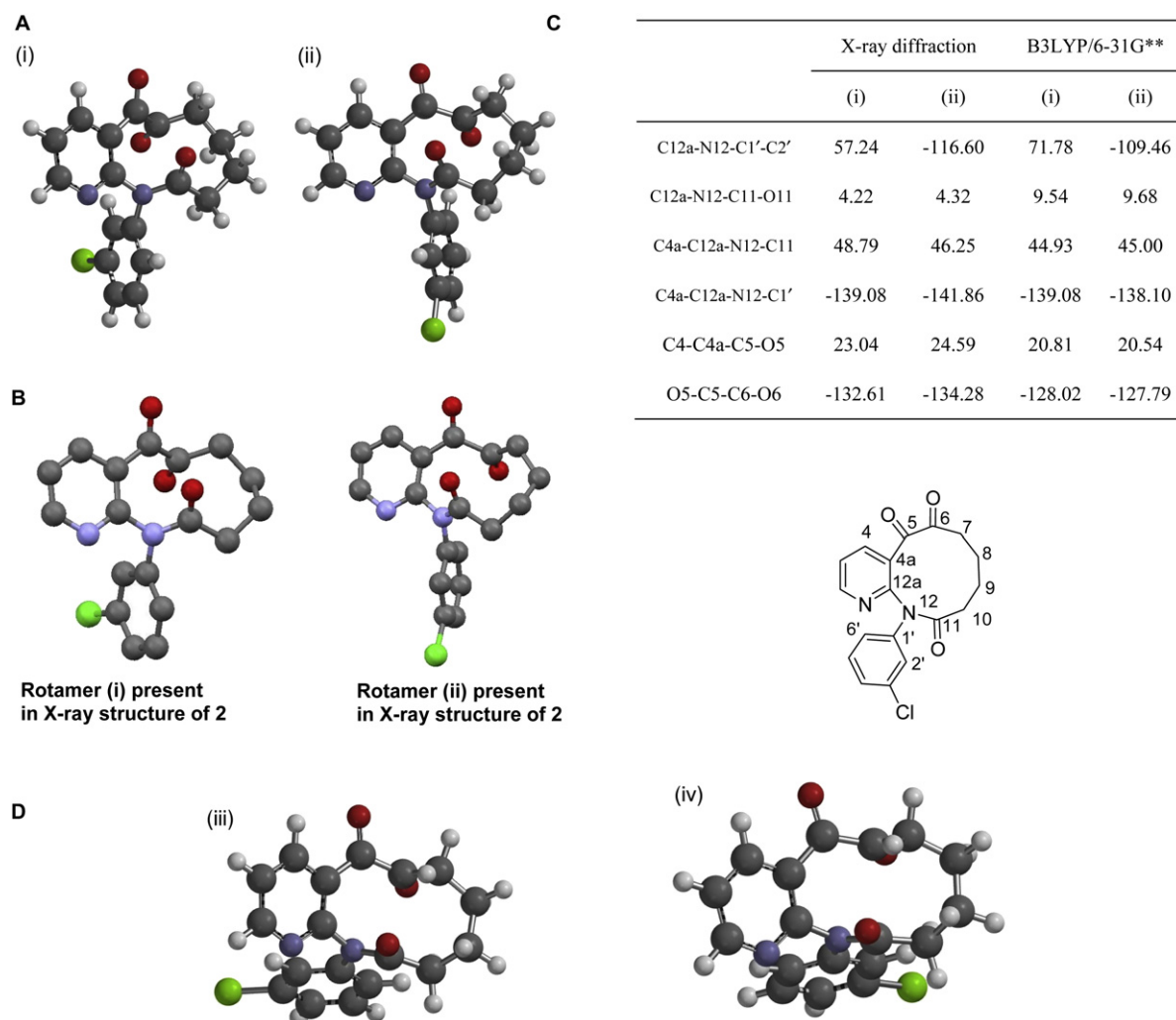
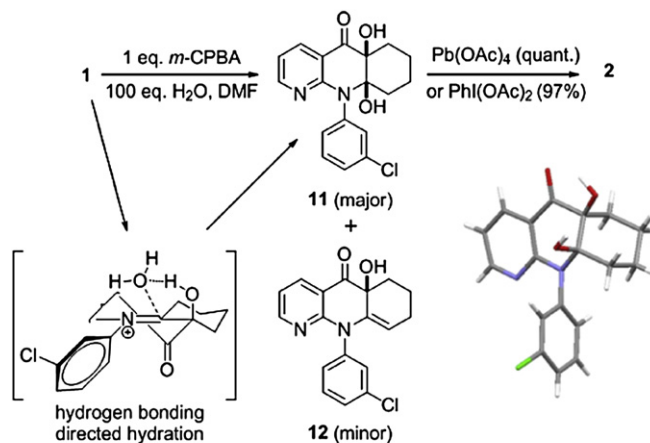


Fig. 2. **A** Ground state structures of **2** calculated at the B3LYP/6-31G** level of theory. **B** The analogous two rotamers observed on X-ray crystallographic analysis of **2**. **C** Comparison of the torsion angles in ° for structures (i) and (ii) of **2** determined and calculated (see Fig. 2A) and the numbering system used for **2**. The values are in relatively close agreement. **D** The two transition states ((iii) and (iv)) for restricted rotation about the N(12)–C(1') bond in **2**.

3. Reinvestigation of the reaction of compound **1** with *m*-CPBA

We next turned our attention to the reported conversion of **1** to **5** (Scheme 1).³ Compound **1** was proposed to react with 1 equiv of *m*-CPBA to give iminium ion **3**. Reaction of **3** with water was then proposed to lead to *anti*-diol **6** (Scheme 1), which was converted to **5** via a retro-aldol reaction. The reported analytical data for **5** included some ¹³C data, IR, MS and microanalysis.³ In our hands, the procedure described for the synthesis of **5** repeatedly gave two main products in addition to recovered **1**. The structure of the major product was assigned as *syn*-diol **11** based on X-ray crystallographic analysis (Scheme 3).⁹ The ¹³C NMR spectrum of **11** in CDCl₃ showed a carbonyl resonance was present at 197.9 ppm,¹⁰ 0.1 ppm different from that quoted in the literature for the C5 carbonyl ¹³C NMR resonance in the proposed product **5**.³ Mass spectroscopic analysis of **11** was consistent with the structural assignment **11** or **5**, as they are isomers. The IR stretch associated with the carbonyl group in **11** was observed at ν 1665 cm⁻¹ (compared with (ν 1685 cm⁻¹) reported **5**). In addition, a broad signal assigned to the presence of an OH group in **11** was observed at ν 3482 cm⁻¹ whereas the reported signals in this region for **5** were ν 3530 and 3460 cm⁻¹. The colourless crystals of **11** obtained by us, changed to yellow crystals on prolonged exposure to air, in accordance with the description

provided for **5** in the literature.³ Interestingly, in our hands, the minor product we obtained in this reaction was also a yellow compound. Extensive 2D NMR analysis of the minor product resulted in its structural assignment as the enamine **12** formed via dehydration of **11**.¹⁰ Interestingly, in the case of **12**, an IR signal was



Scheme 3. Conversion of **1** to *syn*-diol **11** (X-ray structure) and enamine **12**.

observed at ν 1684 cm^{-1} , one wavenumber away from the value reported for the apparently unstable **5**.³

The chemical reactivity of **11** was as expected for a *syn*-diol with rapid and quantitative conversion of **11** to **2** occurring on treatment with either lead tetraacetate¹¹ in dichloromethane at 0 °C or phenyliododiacetate (97% yield, Scheme 3).¹² Amongst several possible explanations for the highly stereoselective formation of *syn*-diol **11** on treatment of **1** with *m*-CPBA and water, we currently favour the hydrogen-bond directed addition of water to the reactive iminium ion **3** to give **11** directly (Scheme 3). This proposal would be in line with previous literature reports.¹³

One possible explanation for the observed difference in the reaction outcome in our hands compared to the literature may be the purity of the *m*-CPBA used in these reactions.¹⁴ The major contaminant in *m*-CPBA, apart from water,¹⁵ is likely to be the corresponding carboxylic acid (*m*-CBA) and so attempts were made to repeat this reaction in the presence of additional *m*-CBA or an alternative acid, trifluoroacetic acid. In both cases only the formation of **11** and increased amounts of **12** were observed. To date we have been unable to detect the formation of **5** under any reaction conditions.

If the mechanism proposed in Scheme 3 is correct, it might also be expected that *m*-CPBA adds to give *syn*-**4** (Fig. 3A) as opposed to *anti*-**4** (Scheme 1). Whilst isomerisation of *syn*-**4** to *anti*-**4** is clearly feasible,¹⁵ and Grob-fragmentation of *anti*-**4** is the most likely method by which **2** can be accessed, it remains possible that **2** is formed via *syn*-**4** as the two bonds that would break during fragmentation can adopt an *anti*-periplanar arrangement in *syn*-**4**. If formation of **2** does occur via *syn*-**4** and the conformation of the 10-

membered ring is rigid, as suggested by VT ¹H NMR (see discussion above), then it would initially be expected to give the 3 carbonyl groups in the relative orientation shown in **2a** (Fig. 3A), that is, different from the orientation **2b** seen in the crystal structure of **2** (Fig. 2B).⁹ However, according to computational studies at the B3LYP/6-31G** level of theory, **2a** is some 36.0 kJ mol⁻¹ higher in energy than **2b**. Attempts to calculate a pathway by which **2a** could be converted to **2b**, (for example, by flipping of the C5–C6 dicarbonyl functionality) were made. Using the semi-empirical RM1 method, the torsion angle O5–C5–C6–O6 was driven in 2° steps from +140° to –140°. Unsurprisingly, the maximum energy structure was located when the O5–C5–C6–O6 torsion angle was approaching 0°, that is, when the dipoles associated with two carbonyl groups are aligned. The maximum energy structure was used as an initial guess for refinement of the transition state structure at the B3LYP/6-31G** level of theory. The calculated ground and transition state structures together with the corresponding O5–C5–C6–O6 torsion angles and relative energies are shown in Fig. 3B. The Gibbs free energy of activation (ΔG^\ddagger_{298} = 41.5 kJ mol⁻¹) calculated for this process using standard methods suggests that flipping of the C5–C6 dicarbonyl functionality in **2a** to give **2b** can occur very readily at room temperature with a half life of **2a** of 1.2×10^{-6} s.

Ruthenium-based reagents are known for their ability to cleave, epoxidise and dihydroxylate alkenes,¹⁶ although to the best of our knowledge reagents of this type have very rarely been used in conjunction with β -enaminones of the general type discussed here.¹⁷ Interestingly, it proved possible to convert **1** to **2** in reasonable yield using ruthenium tetroxide, generated in situ by

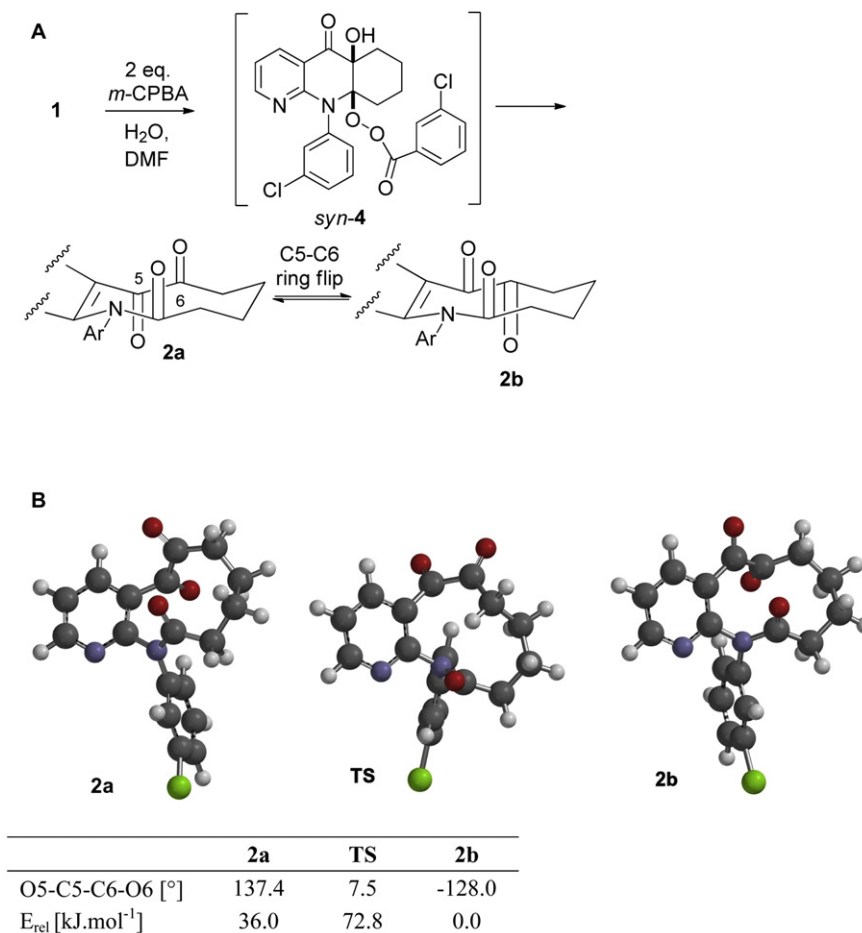


Fig. 3. **A** An alternative proposal for the mechanism of the conversion of **1** to **2** via *syn*-**4**. **B** Ball and stick representations of ground state (**2a** and **2b**) and transition state (**TS**) for flipping of C5–C6 dicarbonyl functionality. The table shows corresponding O5–C5–C6–O6 torsion angles and relative energies.

reaction of $\text{RuCl}_3 \cdot x\text{H}_2\text{O}$ (0.5 mol %) with sodium periodate (6.0 equiv) as the oxidant.¹⁸ Attempts to analyse the progress of this reaction at early time points and in the presence of lower quantities of sodium periodate led to the observation that *syn*-diol **11** was the major product. As **11** has been shown by us to be readily cleaved to **2** by sodium periodate (as well as lead tetraacetate and phenyl-iododiacetate, Scheme 3), it seems very likely that **2** is formed from **1** not by ruthenium-catalysed direct cleavage of the double bond in **1**,¹⁹ but by either direct dihydroxylation of **1** or by epoxidation of **1** by RuO_4 followed by epoxide opening to give **11** (Fig. 3A).

4. Conclusion

The synthesis of compounds containing medium-sized rings remains a challenge. One robust approach for their synthesis involves the use of oxidative cleavage reactions in which the central double bond in a polycyclic compound is cleaved. A previously reported example of this approach involves the fragmentation of the anti-psoriasis drug **1** resulting in the formation of **2**, a compound containing a highly functionalised 10-membered ring. Here we have revisited this report and extended the level of understanding associated with this reaction. In Part II of this study,⁶ the nature of the non-classical stereogenic axis in this system is explored through the use of ring-expanded analogues of **2**.

5. Experimental¹⁰

5.1. 1 10-(3-Chlorophenyl)-6,8,9,10-tetrahydrobenzo[b][1,8]naphthyridin-5(7H)-one^{3,7}

A solution of triethylamine (4.81 mL, 34.5 mmol, 1.10 equiv) and **9** (5.21 g, 34.5 mmol, 1.10 equiv) in toluene (18.0 mL) was added dropwise over 10 min to a stirred, cooled (ice-acetone, -10°C bath) suspension of the crude acid chloride **8** (8.35 g, 31.4 mmol, 1.00 equiv) in toluene (140 mL). As the solid dissolved the dark red reaction mixture was kept between -5°C and $+5^\circ\text{C}$ for 2 h. The reaction mixture was allowed to warm to room temperature over 30 min and then heated at 80°C for 4 h. The reaction mixture was allowed to cool and to stand at room temperature for 12 h, after which the toluene was removed under reduced pressure. The residue was dissolved in dichloromethane (150 mL) and the solution was washed with H_2O (100 mL), 1.0 M $\text{HCl}_{(\text{aq})}$ (100 mL), 1.0 M $\text{Na}_2\text{CO}_{3(\text{aq})}$ (100 mL) and H_2O (100 mL). Aqueous extracts were back extracted with dichloromethane (2×150 mL), and the combined organic portion was dried over Na_2SO_4 , filtered and evaporated. The residue was purified by column chromatography over silica gel (3:2, ethyl acetate/hexane). An analytically pure sample of **1** (5.27 g, 17.0 mmol, 54%) was obtained as a cream solid by recrystallisation from acetonitrile. Mp $187\text{--}188^\circ\text{C}$ (lit.³, $199\text{--}201^\circ\text{C}$); ^1H NMR (300 MHz, CDCl_3): δ 8.84 (dd, $^3J=8.0$ Hz, $^4J=2.0$ Hz, 1H, C4–H), 8.62 (dd, $^3J=4.5$ Hz, $^4J=2.0$ Hz, 1H, C2–H), 7.62–7.60 (m, 2H, Ar–H), 7.38–7.34 (m, 2H, Ar–H, C3–H), 7.29–7.23 (m, 1H, Ar–H), 2.85–2.80 (m, 2H, C6–H₂), 2.42–2.36 (m, 2H, C9–H₂), 1.88–1.81 (m, 4H, C7–H₂, C8–H₂); ^{13}C NMR (75.5 MHz, CDCl_3): δ 177.6 (C5), 152.0 (C2), 151.2 (C10a), 149.1 (C9a), 139.9 (C1'), 135.6 (C4), 135.3 (C3'), 130.6 (Ar), 129.8 (Ar), 129.4 (Ar), 127.7 (Ar), 119.9 (C4a), 119.3 (C3), 118.6 (C5a), 29.6 (C6), 22.5 (C7 and C8), 21.4 (C9); LRMS (ES^+): m/z (%) 311.79 (100) [$\text{M}^{35}\text{Cl}+\text{H}$]⁺.

5.2. 2 12-(3-Chlorophenyl)-7,8,9,10-tetrahydropyrido[2,3-b]azecine-5,6,11(12H)-trione³

Method 1: To a solution of **1** (310 mg, 1.00 mmol) in anhydrous dichloromethane (16.0 mL) was added portion-wise *m*-CPBA (345 mg, 2.00 mmol, 2.00 equiv) and the reaction was stirred at room temperature for 40 h. The reaction mixture was washed with

1.0 M $\text{Na}_2\text{CO}_{3(\text{aq})}$ (10.0 mL) and H_2O (10.0 mL). The aqueous washes were back extracted with dichloromethane (2×30.0 mL). The combined organic phase was dried (MgSO_4), filtered and concentrated in vacuo. The residue was purified by column chromatography over silica gel (1:1, ethyl acetate/hexane). An analytically pure sample of **2** (223 mg, 0.652 mmol, 65%) was obtained as yellow needles by recrystallisation from ethanol.

Method 2: Sodium periodate (642 mg, 3.00 mmol, 6.00 equiv) was stirred in H_2O (0.750 mL) and 2 N sulfuric acid (100 μL). After the solid had dissolved, the solution was cooled to 0°C . Ruthenium (III) chloride hydrate (0.622 mg, 0.003 mmol, 0.5 mol %) was then added and the reaction was stirred until the colour turned bright yellow. Ethyl acetate (3.00 mL) and acetonitrile (3.00 mL) were added and stirring was continued for a further 5 min. Compound **1** (155 mg, 0.500 mmol, 1.00 equiv) was then added to the reaction and the slurry was stirred at room temperature for 24 h. The reaction mixture was poured into a mixture of saturated NaHCO_3 solution (10.0 mL) and saturated sodium thiosulfate solution (10.0 mL). The phases were separated, and the aqueous layer was extracted with ethyl acetate (3×20.0 mL). The combined organic layers were dried (Na_2SO_4) and concentrated in vacuo. The crude product was purified by flash column chromatography using silica gel (1:9–3:7, ethyl acetate/hexane), which afforded two fractions. The fraction eluting at 1:9 ethyl acetate/hexane was **2** (68.4 mg, 0.200 mmol, 40%) as a yellow solid. The fraction eluting at 3:7 ethyl acetate/hexane was **11** (103 mg, 0.300 mmol, 60%) as a cream solid.

Method 3: To a cooled solution of **11** (20.6 mg, 0.0600 mmol, 1.00 equiv) in anhydrous DCM (5.00 mL) at 0°C (ice/water bath) was added lead tetraacetate (53.2 mg, 0.120 mmol, 2.00 equiv) and the reaction was stirred for 20 min. The solvent was removed in vacuo and the crude residue was purified by flash column chromatography over silica gel (2:3, ethyl acetate/hexane) to afford **2** (20.5 mg, 0.060 mmol, 99%) as a yellow solid.

Method 4: To a solution of **11** (127 mg, 0.370 mmol, 1.00 equiv) in anhydrous dichloromethane (10 mL) was added portion-wise (diacetoxyiodo)benzene (238 mg, 0.740 mmol, 2.00 equiv) and the reaction was stirred at room temperature for 1 h. The reaction mixture was washed with a saturated NaHCO_3 solution (10.0 mL) and a saturated sodium thiosulfate solution (10.0 mL). The aqueous washes were back extracted with dichloromethane (2×30.0 mL) and the combined organic phase was dried (MgSO_4), filtered and concentrated in vacuo. The residue was purified by flash column chromatography over silica gel (2:3, ethyl acetate/hexane) to afford **2** (123 mg, 0.360 mmol, 97%) as a yellow solid.

Mp $157.5\text{--}157.9^\circ\text{C}$ (lit.³, $173\text{--}175^\circ\text{C}$); ^1H NMR (300 MHz, CDCl_3): δ 8.49 (dd, $^3J=5.0$ Hz, $^4J=2.0$ Hz, 1H, C2–H), 8.28 (dd, $^3J=8.0$ Hz, $^4J=2.0$ Hz, 1H, C4–H), 7.43–7.34 (m, 3H, Ar–H), 7.31–7.27 (m, 1H, C3–H), 7.26–7.21 (m, 1H, Ar–H), 3.33–3.25 (m, 1H, C7–H_a), 2.56–2.50 (m, 1H, C7–H_b), 2.43–2.38 (m, 1H, C10–H_a), 2.16–2.04 (m, 2H, C10–H_b, C9–H_a), 1.95–1.82 (m, 2H, C9–H_b, C8–H_a), 1.76–1.66 (m, 1H, C8–H_b); ^{13}C NMR (75.5 MHz, CDCl_3): δ 202.1 (C6), 190.5 (C5), 176.1 (C11), 153.1 (C12a), 152.7 (C2), 142.4 (C1'), 139.5 (C4), 135.5 (C3'), 130.7 (Ar), 129.0 (Ar), 128.7 (Ar), 127.1 (Ar), 125.2 (C4a), 122.1 (C3), 37.6 (C7), 36.0 (C10), 25.5 (C9), 25.2 (C8); IR (KBr): $\nu_{\text{max}}=2951$ (m), 2870 (w), 1701 (s), 1684 (s), 1653 (s), 1592 (m), 1424 (m), 1287 (m), 1160 (w), 760 (m) cm^{-1} ; LRMS (ES^+): m/z (%) 365.10 (100) [$\text{M}^{35}\text{Cl}+\text{Na}$]⁺; HRMS (ES^+): m/z calcd for $\text{C}_{18}\text{H}_{15}^{35}\text{ClN}_2\text{NaO}_3$ [$\text{M}^{35}\text{Cl}+\text{Na}$]⁺: 365.0669; found 365.0666.

5.3. 7 2-((3-Chlorophenyl)amino)-3-pyridinecarboxylic acid²⁰

A mixture of 2-chloronicotinic acid (15.8 g, 100 mmol, 1.00 equiv), 3-chloroaniline (25.5 g, 200 mmol, 2.00 equiv), *p*-toluenesulfonic acid $\cdot \text{H}_2\text{O}$ (1.90 g, 10.0 mmol, 0.100 equiv) and H_2O (100 mL) was heated at reflux for 4 h. The cooled mixture was filtered, and the collected yellow precipitate was washed with cold

H₂O (2×50.0 mL) and dried overnight (60 °C) in an oven to afford the title compound **7** (24.1 g, 970 mmol, 97%) as a bright yellow solid. Mp 195–196 °C (lit.²⁰, 199–201 °C); ¹H NMR (300 MHz, CD₃OD): δ 8.43–8.36 (m, 2H, C6–H, C4–H), 8.03 (dd, ⁴J=2.0, 2.0 Hz, 1H, C2'–H), 7.48–7.44 (m, 1H, C5'–H), 7.35–7.28 (m, 1H, C6'–H), 7.09–7.04 (m, 1H, C4'–H), 6.91 (dd, ³J=7.5, 5.0 Hz, 1H, C5–H); IR 3059 (s), 1671 (s), 1567 (m), 1426 (m), 1241 (m), 1094 (m), 763 (m) cm^{−1}; LRMS (ES[−]): *m/z* (%) 247.67 (100) [M³⁵Cl–H][−].

5.4. 8-2-((3-Chlorophenyl)amino)-3-pyridinecarbonyl chloride^{7b}

2-((3-Chlorophenyl)amino)-3-pyridinecarboxylic acid **7** (8.18 g, 33.0 mmol, 1.0° equiv) was added to thionyl chloride (13.3 mL, 182 mmol, 5.50 equiv) and DMF (catalytic 100 μL) and stirred at 25 °C for 1 h. Concentration of the reaction mixture in vacuo afforded the crude acid chloride **8** (8.35 g, 31.4 mmol, 96%), which was used without further purification. ¹H NMR (300 MHz, CDCl₃): δ 9.65 (s, NH), 8.51 (dd, ³J=4.5 Hz, ⁴J=2.0 Hz, 1H, C6–H), 8.46 (s, 1H, C4–H), 7.85 (br s, 1H, C2'–H), 7.50–7.25 (m, 3H, C5'–H, C6'–H, C4'–H), 6.92 (dd, ³J=7.5, 4.5 Hz, 1H, C5–H).

5.5. 11 (5a*S*, 9a*R*)-10-(3-Chlorophenyl)-5a,9a-dihydroxy-6,7,8,9,9a,10-hexahydrobenzo[*b*][1,8]-naphthyridin-5(5a*H*)-one

Method 1: To a solution of **1** (311 mg, 1.00 mmol, 1.00 equiv) in dimethyl formamide (6.00 mL) diluted with H₂O (2.00 mL) was added purified *m*-CPBA (173 mg, 1.00 mmol, 1.00 equiv) and the reaction was stirred at room temperature for 94 h. The reaction mixture was poured into H₂O (100 mL) and extracted with ethyl acetate (3×150 mL). The combined organic extracts were washed with H₂O (100 mL), 1.0 M NaHCO₃(aq) solution (100 mL) and brine (100 mL), dried (MgSO₄) and concentrated in vacuo to give a yellow oil. Purification by column chromatography using silica gel (1:10–4:6, ethyl acetate/hexane) afforded three fractions. The fraction eluting at 1:10 ethyl acetate/hexane was **11** (110 mg, 0.320 mmol, 32%) as a white solid. The fraction eluting at 15:85 ethyl acetate/hexane was **12** (48.9 mg, 0.150 mmol, 15%) as a yellow oil. The fraction eluting at 4:6 ethyl acetate/hexane was the starting pyridinone **1** (164 mg, 0.530 mmol, 53%) as a cream solid. This experiment was also repeated using an unpurified batch of *m*-CPBA. No change in the products identified from this reaction was observed. In addition attempts to purify either the crude reaction by column chromatography eluting with MeOH/DCM (1:99) yielded the same products as when ethyl acetate/hexane mixtures were used.¹⁵ Repurification of **11** by column chromatography eluting with MeOH/DCM (1:99) yielded only **11**.¹⁵

Method 2: Sodium periodate (321 mg, 1.50 mmol, 3.00 equiv) was stirred in H₂O (0.750 mL) and 2 N sulfuric acid (100 μL). After the solid had dissolved, the solution was cooled to 0 °C. Ruthenium (III) chloride hydrate (0.622 mg, 0.00300 mmol, 0.5 mol %) was then added and the reaction was stirred until the colour turned bright yellow. Ethyl acetate (3 mL) and acetonitrile (3 mL) were added and stirring was continued for a further 5 min. Compound **1** (155 mg, 0.500 mmol, 1.00 equiv) was then added to the reaction and the slurry was stirred at room temperature for 24 h. The reaction mixture was poured into a mixture of saturated NaHCO₃ solution (10.0 mL) and saturated sodium thiosulfate solution (10.0 mL). The phases were separated, and the aqueous layer was extracted with ethyl acetate (3×20.0 mL). The combined organic layers were dried (Na₂SO₄) and concentrated in vacuo. The crude product was purified by flash column chromatography using silica gel (2:3, ethyl acetate/hexane) to afford **11** (127 mg, 0.370 mmol, 74%) as a white solid.

Mp 167.1–168 °C; ¹H NMR (400.1 MHz, CDCl₃): δ 8.32–8.27 (m, 1H, C2–H), 8.16 (dd, ³J=7.6 Hz, ⁴J=1.9 Hz, 1H, C4–H), 7.63–7.60 (m, 0.5H, C2'–H), 7.52–7.47 (m, 0.5H, C6'–H), 7.44–7.35 (m, 2.5H, C5'–H, C4'–H, C2'–H), 7.34–7.30 (m, 0.5H, C6'–H), 6.83 (dd, ³J=7.6, 1.9 Hz, 1H, C3–H), 4.02 (s, 1H, C5a–OH), 3.07 (s, 1H, C9a–OH), 2.00–1.89 (m, 1H, C6–H_a), 1.81–1.46 (m, 7H, C9–H₂, C8–H₂, C6–H_b, C7–H₂); ¹³C NMR (100.1 MHz, CDCl₃, 298 K): δ 198.1 (C5), 158.7 (C10a), 155.6 & 155.5 (C1), 141.2 (C1'), 136.6 (2×C4), 135.1 & 134.0 (C3'), 131.9 (C5'), 130.5 (C4'), 130.0 (C2'), 129.8 (C6'), 129.4 (C5'), 128.1 (C4'), 128.1 (C6'), 128.0 (C2'), 115.7 (C3), 111.6 & 111.5 (C4a), 89.5 (C9a), 77.3 (C5a), 33.6 (2×C6), 32.9 & 32.8 (C9), 22.2 & 22.1 (C7), 18.9 (2×C8); IR (KBr): ν_{max}=3482 (s) (OH), 2926 (s) (CH₂), 2944 (s) (CH₂), 2865 (m) (CH₂), 1665 (s) (C=O), 1598 (m), 1470 (m), 1196 (m) (C–O), 722 (m) (C–Cl) cm^{−1}; LRMS (ES⁺): *m/z* (%) 367.04 (100) [M³⁵Cl+Na]⁺; HRMS (ES⁺): *m/z* calcd for C₁₈H₁₇³⁵ClN₂ NaO₃ [M³⁵Cl+Na]⁺: 367.0825; found 367.0827.

5.6. 12 (5*S*)-10-(3-Chlorophenyl)-5a-hydroxy-5a,6,7,8-tetrahydrobenzo[*b*][1,8]naphthyridin-(10*H*)-one

¹H NMR (300 MHz, CDCl₃): δ 8.27 (dd, ³J=4.7 Hz, ⁴J=2.1 Hz, 1H, C2–H), 8.18 (m, ³J=7.7 Hz, ⁴J=2.1 Hz, 1H, C4–H), 7.45 (dd, ³J=7.5, 7.6 Hz, 1H, C5'–H), 7.40–7.37 (m, 1H, C4'–H), 7.30 (dd, ⁴J=2.0, 2.0 Hz, 1H, C2'–H), 7.19 (ddd, ³J=7.5 Hz, ⁴J=2.0, 1.3 Hz, 1H, C6'–H), 6.82 (dd, ³J=7.7, 4.7 Hz, 1H, C3–H), 5.11 (dd, ³J=5.7 Hz, ⁴J=3.1 Hz, 1H, C9–H), 2.45 (br s, 1H, OH), 2.27–1.91 (m, 4H, C6–H₂, C8–H₂), 1.87–1.47 (m, 2H, C7–H₂); ¹³C NMR (75.5 MHz, CDCl₃): δ 192.1 (C5), 154.7 (C10a), 154.6 (C2), 141.9 (C1'), 139.4 (C9a), 137.5 (C4), 135.3 (C3'), 130.8 (C5'), 130.3 (C2'), 128.3 (C6'), 128.2 (C4'), 119.4 (C9), 115.6 (C3), 112.4 (C4a), 69.6 (C5a), 30.2 (C6), 25.3 (C8), 18.0 (C7); IR (KBr): ν_{max}=3484 (s) (OH), 2945 (m) (CH₂), 1684 (s) (C=O), 1567 (m), 1361 (m), 1174 (m) (C–O), 748 (m) (C–Cl) cm^{−1}; LRMS (ES⁺): *m/z* (%) 349.04 (100) [M³⁵Cl+Na]⁺; HRMS (ES⁺): *m/z* calcd for C₁₈H₁₅³⁵ClN₂NaO₂ [M³⁵Cl+Na]⁺: 349.0725; found 349.0724. Repurification of **12** by column chromatography eluting with MeOH/DCM (1:99) yielded only **12**.¹⁵

Acknowledgements

The authors thank BBSRC (A.M.J.) and the Royal Society (Research Fellowship to N.J.W.) for funding.

Supplementary data

VT NMR data, 2D NMR spectra associated with **2** and **12**, low temperature NMR assignment for **11**, general and computational experimental and ¹H and ¹³C NMR spectra of all new compounds. Supplementary data related to this article can be found online at doi:10.1016/j.tet.2010.10.044.

References and notes

- For recent reviews see: (a) Constantieux, T.; Rodriguez, J. *Sci. Synth.* **2005**, 26, 413–462; (b) Roxburgh, C. J. *Tetrahedron* **1993**, 49, 10749–10784; (c) Staach, H.; Hesse, M. *Tetrahedron* **1988**, 44, 1573–1590.
- For detailed discussion of atropisomerism see: (a) Oki, M. *Recent Advances in Atropisomerism*, 1st ed.; John Wiley: New York, NY, 1983; (b) Clayden, J. *Angew. Chem., Int. Ed.* **1997**, 36, 949–951; (c) Clayden, J.; Moran, W. J.; Edwards, P. J.; LaPlante, S. R. *Angew. Chem., Int. Ed.* **2009**, 48, 2–6.
- Friary, R. J.; Schwerdt, J. H. *Tetrahedron* **1991**, 47, 9981–9984.
- Friary, R. J.; Spangler, M.; Osterman, R.; Schulman, L.; Schwerdt, J. H. *Chirality* **1996**, 8, 364–371.
- Grob, C. A. *Angew. Chem., Int. Ed. Engl.* **1969**, 8, 535–622.
- Lebl, T.; Jones, A. M.; Lorion, M. M.; Slawin, A. M. Z.; Philp, D.; Westwood, N. J. *Tetrahedron* **2010**.
- (a) Friary, R. J.; Seidl, V.; Schwerdt, J. H.; Chan, T.-M.; Cohen, M. P.; Conklin, E. R.; Duelfer, T.; Hou, D.; Nafissi, M.; Runkle, R. L.; Tahbaz, P.; Tiberi, R. L.; McPhail, A. T. *Tetrahedron* **1993**, 49, 7179–7192; (b) Friary, R. J.; Seidl, V.; Schwerdt, J. H.; Cohen, M. P.; Hou, D.; Nafissi, M. *Tetrahedron* **1993**, 49, 7169–7178; (c) In our

- hands there was a considerable difference in the melting point of **1** compared with the value reported previously.³
8. A discrepancy in the melting point of **2** prepared by us and that reported previously³ was observed.
9. Crystallographic data (excluding structure factors) for **2** and *syn*-**11** has been deposited with the Cambridge Crystallographic Data Centre as supplementary publication no. CCDC 741362 and 741363. Copies of the data can be obtained, free of charge, on application to CCDC, 12 Union Road, Cambridge CB2 1EZ, UK, (fax: +44(0)1223 336033 or e-mail: deposit@ccdc.cam.ac.uk).
10. For a more detailed discussion see [Supplementary data](#).
11. Lead tetraacetate is known to undergo both a concerted fragmentation that is rapid with *syn*-diols and also a much slower reaction to cleave *anti*-diols. The speed of the reaction reported here was consistent with the structure of *syn*-diol **11**. For a recent example of the use of lead tetraacetate to cleave a *syn*-diol in the context of natural product synthesis see Makiyi, E. F.; Frade, R. F. M.; Lebl, T.; Jaffray, E. G.; Cobb, S. E.; Harvey, A. L.; Slawin, A. M. Z.; Hay, R. T.; Westwood, N. J. *Eur. J. Org. Chem.* **2009**, 33, 5711–5715.
12. (a) Huang, S.; Wang, F.; Gan, L.; Yuan, G.; Zhou, J.; Zhang, S. *Org. Lett.* **2006**, 8, 277–279; (b) Xiao, Z.; Yao, J.; Yang, D.; Wang, F.; Huang, S.; Gan, L.; Jia, Z.; Jiang, Z.; Yang, X.; Zheng, B.; Yuan, G.; Zhang, S.; Wang, Z. *J. Am. Chem. Soc.* **2007**, 129, 16149–16162.
13. (a) Davies, S. G.; Key, M.-S.; Rodriguez-Solla, H.; Sanganee, H. J.; Savory, E. D.; Smith, A. D. *Synlett* **2003**, 1659–1662; (b) Aciro, A.; Davies, S. G.; Garner, A. C.; Ishii, Y.; Key, M.-S.; Ling, K. B.; Prasad, R. S.; Roberts, P. M.; Rodriguez-Solla, H.; O'Leary-Steele, C.; Russell, A. J.; Sanganee, H. J.; Savory, E. D.; Smith, A. D.; Thomson, J. E. *Tetrahedron* **2008**, 64, 9320–9344.
14. In our hands *m*-CPBA was purified prior to use according to the procedure of Armarego, W. L. F.; Chai, C. L. *Purification of Laboratory Chemicals*, 5th ed.; Butterworth-Heinemann: Oxford, UK, 2003.
15. We thank the reviewers for raising these issues during the assessment of this manuscript. We would also like to thank the authors of Ref. 3 for help and advice throughout the review process.
16. For a recent review of the chemistry of RuO₄ see Plietker, B. – *Synthesis* **2005**, 15, 2453–2472; For a recent review of the use of ruthenium-based catalysed in epoxidation reactions see Chatterjee, D. *Coord. Chem. Rev.* **2008**, 252, 176–198.
17. Ramesh, N. G.; Klunder, A. J. H.; Zwanenberg, B. *Tetrahedron Lett.* **2001**, 42, 7707–7709.
18. Plietker, B.; Niggemann, M. *Org. Lett.* **2003**, 5, 3353–3356.
19. Frunzke, J.; Loschen, C.; Frenking, G. *J. Am. Chem. Soc.* **2004**, 126, 3642–3652.
20. Sherlock, M. H.; Kaminski, J. J.; Tom, W. C.; Lee, J. F.; Wong, S. C.; Kreutner, W.; Bryant, R. W.; McPhail, A. T. *J. Med. Chem.* **1988**, 31, 2108–2121.